Developmental Cell
Article

Reverse Genetic Screening Reveals Poor Correlation between Morpholino-Induced and Mutant Phenotypes in Zebrafish

Fatma O. Kok,[1,7] Masahiro Shin,[1,7] Chih-Wen Ni,[1,7,8] Ankit Gupta,[1] Ann S. Grosse,[1] Andreas van Impel,[2] Bettina C. Kirchmaier,[2,9] Josi Peterson-Maduro,[2] George Kourkoulis,[1] Ira Male,[1] Dana F. DeSantis,[1] Sarah Sheppard-Tindell,[1] Lwaki Ebarasi,[3,4] Christer Betsholtz,[3,4] Stefan Schulte-Merker,[2,5] Scot A. Wolfe,[1,6] and Nathan D. Lawson[1,*]

[1]Program in Gene Function and Expression, University of Massachusetts Medical School, Worcester, MA 01605, USA
[2]Hubrecht Institute, 3584CT Utrecht, the Netherlands
[3]Department of Immunology, Genetics, and Pathology, Rudbeck Laboratory, Uppsala University, 751 85 Uppsala, Sweden
[4]Department of Medicinal Biochemistry and Biophysics, Karolinska Institute, 171 77 Stockholm, Sweden
[5]Institute for Cardiovascular Organogenesis and Regeneration, Cells-in-Motion Cluster of Excellence, University of Münster, 48149 Münster, Germany
[6]Department of Biochemistry and Molecular Pharmacology, University of Massachusetts Medical School, Worcester, MA 01605, USA
[7]Co-first author
[8]Present address: Department of Biomedical Engineering, Khalifa University of Science, Technology and Research (KUSTAR), PO Box 127788, Abu Dhabi, United Arab Emirates
[9]Present address: Institute of Cell Biology and Neuroscience and Buchmann Institute for Molecular Life Sciences (BMLS), University of Frankfurt, 60438 Frankfurt am Main, Germany
*Correspondence: nathan.lawson@umassmed.edu
http://dx.doi.org/10.1016/j.devcel.2014.11.018

SUMMARY

The widespread availability of programmable site-specific nucleases now enables targeted gene disruption in the zebrafish. In this study, we applied site-specific nucleases to generate zebrafish lines bearing individual mutations in more than 20 genes. We found that mutations in only a small proportion of genes caused defects in embryogenesis. Moreover, mutants for ten different genes failed to recapitulate published Morpholino-induced phenotypes (morphants). The absence of phenotypes in mutant embryos was not likely due to maternal effects or failure to eliminate gene function. Consistently, a comparison of published morphant defects with the Sanger Zebrafish Mutation Project revealed that approximately 80% of morphant phenotypes were not observed in mutant embryos, similar to our mutant collection. Based on these results, we suggest that mutant phenotypes become the standard metric to define gene function in zebrafish, after which Morpholinos that recapitulate respective phenotypes could be reliably applied for ancillary analyses.

INTRODUCTION

The zebrafish has become a central model system to investigate vertebrate development. Early foundational studies utilized zebrafish in large-scale forward genetic screens to identify mutants affecting different aspects of embryonic development (Driever et al., 1996; Haffter et al., 1996). These studies took advantage of the many benefits of zebrafish husbandry and embryogenesis. In particular, rapid external development of the transparent zebrafish embryo allowed detection of a range of mutant phenotypes during development. The hardy nature of zebrafish adults and their ability to produce large clutch sizes facilitated subsequent mapping of causative mutant genes (Lawson and Wolfe, 2011). These genetic screens, based simply on observing embryonic morphology, resulted in the discovery of genes required for distinct steps in embryogenesis, including gastrulation (Hammerschmidt et al., 1996), cardiovascular morphogenesis (Stainier et al., 1996), and hematopoiesis (Ransom et al., 1996). Subsequent forward genetic screens have been applied to dissect an array of different biological processes, ranging from immunity to digestion (Lawson and Wolfe, 2011). This work demonstrates the broad and powerful impact that the zebrafish has had as a genetic model system across multiple fields of study.

Despite the utility of forward genetics, screening to saturation in the zebrafish is challenging (Lawson and Wolfe, 2011). At the same time, the deluge of sequence data over the past decade has revealed a wealth of genes for which no mutations currently exist in zebrafish. Thus, there is a need for reverse genetic approaches to assess gene function. While not a true genetic approach, the introduction of antisense Morpholino oligomers (MOs) was initially greeted with excitement in the zebrafish community as a tool to interrogate gene function. MOs differ from standard nucleic acid oligonucleotides in that they possess a six-ring heterocycle backbone and nonionic phosphorodiamidate linkages (Summerton and Weller, 1997). These modifications make MOs highly stable in vivo, allow them to have a high affinity for RNA, and supposedly reduce their off-target

binding to macromolecules (Summerton, 2007). MOs can be designed to block translation or splicing and their injection into one-cell stage zebrafish embryos can recapitulate known mutant phenotypes (Draper et al., 2001; Nasevicius and Ekker, 2000). MOs also can block microRNA maturation and their binding to target 3′ untranslated regions (UTRs; Choi et al., 2007; Kloosterman et al., 2007). Thus, MOs provide, in principle, an accessible and straightforward method for gene knockdown in the zebrafish embryo.

Given their ease of use in zebrafish, MOs have enabled widespread analysis of gene function. However, MOs can induce p53-dependent apoptosis (Ekker and Larson, 2001; Pickart et al., 2006; Robu et al., 2007) and off-target cell-type-specific changes in gene expression that confound phenotypic analysis (for example, see Amoyel et al., 2005; Gerety and Wilkinson, 2011). While it is possible to alleviate off-target phenotypes by simultaneously reducing p53 levels (Robu et al., 2007), the mechanism of p53 activation is unknown. Despite this issue, anecdotal claims suggest that MOs do not share the same problems with off-target effects associated with other antisense technology, such as phosphorothioate-modified oligonucleotides (Summerton, 2007). However, there has been little empirical research in this area.

Fortunately, definitive reverse genetic approaches in zebrafish recently have become available. In particular, programmable site-specific nucleases now enable targeted gene disruption in the zebrafish. Initial work utilized zinc finger nucleases (ZFNs; Doyon et al., 2008; Meng et al., 2008), and transcription activator-like effector nucleases (TALENs), which provide improved specificity over ZFNs, also have been developed (Cade et al., 2012). In both cases, mRNAs encoding ZFN or TALEN heterodimers were injected into one-cell stage embryos, where they bound to their target and induced a double strand break. Imprecise repair of this break by nonhomologous end joining introduces small insertions or deletions that can lead to a frameshift when targeting coding sequence; in a proportion of the embryos, such lesions will occur within the germline. More recently, the programmable bacterial nuclease Cas9 has been applied successfully to introduce heritable lesions in the zebrafish genome at high frequency (Hwang et al., 2013). Together, these tools provide a robust means to generate zebrafish bearing targeted mutations in genes of interest.

A number of groups, including our own, have put significant effort toward the development and application of site-specific nucleases in zebrafish (Bedell et al., 2012; Cade et al., 2012; Chen et al., 2013; Dahlem et al., 2012; Gupta et al., 2012, 2013; Hwang et al., 2013; Sander et al., 2011; Zhu et al., 2011). However, the systematic analysis of phenotypes in derived lines has lagged. In this study, we generated and characterized mutant lines for more than 20 genes. We found that the majority of these genes are dispensable for embryonic development. We also did not observe previously published MO-induced (morphant) phenotypes in ten mutant lines. A broader comparison of all published morphant phenotypes with the Sanger Zebrafish Mutation Project (ZMP) revealed similar discrepancies. Taken together, these observations suggest that MO off-target effects are much more prevalent than previously stated. Our results highlight the need to reevaluate the use of antisense-based technology for characterization of gene function in the zebrafish and emphasize the importance of applying targeted gene disruption for this purpose.

RESULTS

Generation of Mutants in Candidate Genes of Interest

Our general goal was to identify novel functions for genes involved in embryonic vascular development. For this purpose, we applied programmable site-specific nucleases to introduce targeted deletions in candidate genes of interest identified from a number of sources (Table S1 available online). For the most part, candidate genes were expressed in endothelial cells based on published studies, available in situ hybridization data at the Zebrafish Information Network (ZFIN), or identified through our own unpublished work (Table S1 and data not shown). Fourteen genes had been targeted by MOs in published work and shown to cause a developmental phenotype, including ten that displayed a vascular or lymphatic defect (*amot*, *ccbe1*, *elmo1*, *ets1*, *flt4*, *fmnl3*, *gata2a*, *mmp2*, *nrp1a*, and *pdgfrb*; Table S1). We have previously reported vascular defects in the *gata2a* mutant (Zhu et al., 2011), and it is included here as the first mutant generated in our knockout pipeline. We also included *ccbe1* and *flt4* as positive control target genes for which vascular defects already have been reported in mutants from forward genetic screens (Hogan et al., 2009a, 2009b).

We applied ZFNs, TALENs, and, in one case, Cas9, to target genomic sequence that harbored a restriction site that could be used for genotyping and encoded amino acids in the amino-terminal half of a protein (Table S2; see below; data not shown). We did not target near the annotated start codon to avoid alternative translational start sites, except when targeting a signal peptide (e.g., *ccbe1* and *mmp2*). We identified founder fish bearing small insertions or deletions in their germline that introduced a frameshift into the coding sequence or eliminated a splice site (Table S2). All of the lesions were expected to truncate the protein and cause non-sense-mediated decay (NMD) of the mRNA transcript (see below; Table S2). For the *linc:birc6* locus, we generated a large segmental deletion. In total, we generated mutant lines bearing 32 distinct lesions in 24 genes (Table S2).

Lack of Embryonic Defects and Discrepancy with Morphant Vascular Phenotypes

We performed all phenotypic analysis on embryos derived from multiple in-crosses of identified heterozygous carriers of a respective mutation. In most cases, we generated families of heterozygous carriers by crossing founders with adults bearing endothelial or lymphatic endothelial transgenes to visualize vascular or lymphatic morphology, respectively (see below). We screened embryos for overt defects between 24 hr postfertilization (hrpf) and 5 days postfertilization. In parallel, we observed vascular morphology in transgenic embryos, and screened for abnormal circulatory patterns, loss of circulation, and evidence of hemorrhage. Following 5 days postfertilization, we genotyped embryos to confirm the presence of homozygous wild-type, mutant, and heterozygous progeny at the expected ratios. In all cases where embryos failed to exhibit phenotypes, we were able to detect genotypically mutant embryos at the expected frequency (data not shown; see examples for *ets1a*, *fam38a*, and *fmnl3* below).

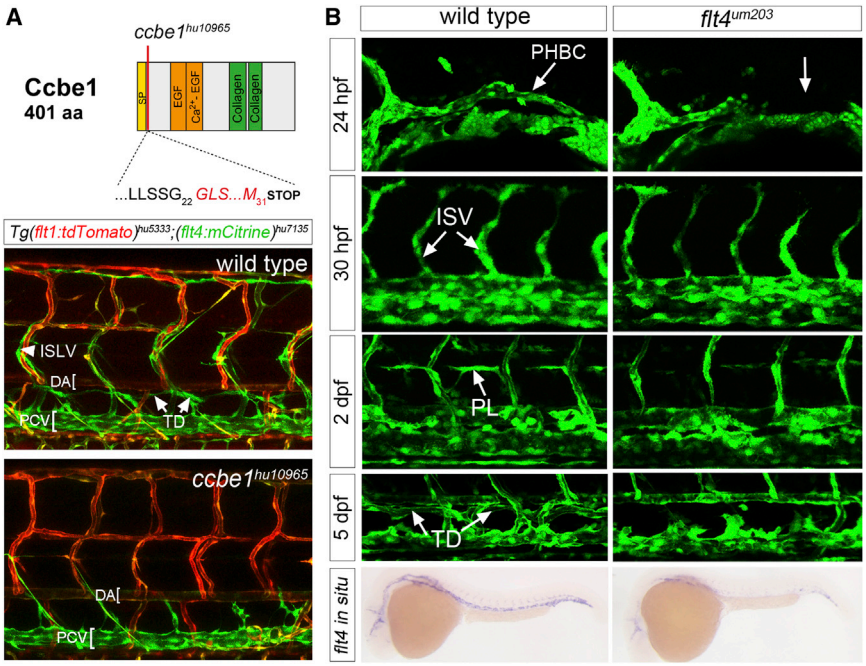

Figure 1. TALEN-Generated Mutations in *ccbe1* and *flt4* Cause Lymphatic Defects

(A) Schematic of Ccbe1 protein indicating position of the *ccbe1*^{hu10965} frameshift. SP, signal peptide; EGF, EGF-like domain; Ca^{2+}-EGF, calcium-binding EGF-like domain; and collagen, collagen-like domain. Images are confocal micrographs of wild-type or *ccbe1*^{hu10965} mutant embryo bearing Tg(*flt4:mCitrine*)^{hu7135} (green) and *Tg*(*flt1:tdTomato*)^{hu5333} (red) transgenes. Homozygous *ccbe1*^{hu10965} mutants lacked the TD and ISLVs at 5 days postfertilization; position of the DA and posterior cardinal vein (PCV) are indicated. Lateral views, anterior to the left, and dorsal is up. (B) Confocal micrographs of *Tg*(*fli1a:egfp*)^{y1} wild-type and *flt4*^{um203} sibling embryos at 24 hrpf, 30 hrpf, 2 days postfertilization, and 5 days postfertilization. Positions of the PHBC, ISVs, PLs, and TD are indicated. All of these structures except ISVs are missing in *flt4*^{um203} mutants at indicated stages (right). (Bottom) *flt4* transcript by whole mount in situ hybridization in wild-type and *flt4*^{um203} mutant embryos at 28 hrpf. Lateral views, anterior to the left, and dorsal is up.

In the course of phenotypic analysis, we observed defects caused by mutations in only 3 of the 24 genes. These included *gata2a*, *ccbe1*, and *flt4* mutants, the latter two of which exhibited loss of the thoracic duct (TD), a primitive lymphatic structure (Figures 1A and 1B), as expected from previous studies (Hogan et al., 2009a, 2009b). The *flt4* mutant embryos also failed to form the primordial hindbrain channel (PHBC) and parachordal lymphangioblasts (PLs; Figure 1B). All other mutants displayed normal overall and vascular morphology as well as circulatory function throughout the first 5 days of development (Figure S1; Table S3; data not shown). For example, within the embryonic trunk at 30 hrpf, intersegmental vessels (ISVs) completed their sprouting from the dorsal aorta (DA) and began to form the dorsal longitudinal anastomotic vessel (DLAV) in wild-type siblings (Figure 2A). The formation of these vessels has been used to screen for genes required for angiogenesis (for examples, see Covassin et al., 2009; Isogai et al., 2003; Lawson and Weinstein, 2002).

We did not observe defects in vascular morphogenesis or circulatory function in any of the other mutant embryos, including those bearing mutations in guanine nucleotide exchange factors, such as *arhgef9b*, *kalrnb*, *fgd5a*, or *prex2* (Figures 2B–2D; Table S3; data not shown), which are candidates for genes important for endothelial migration. Most strikingly, we failed to observe defects in embryos bearing mutations in genes previously shown to be required for ISV formation using MOs (Table 1; Table S3). For example, individual MO knockdowns of *fmnl3* and *pdgfrb* caused a block in ISV sprouting (Hetheridge et al., 2012; Wiens et al., 2010). However, embryos mutant for *fmnl3*^{um150} or *pdgfrb*^{um148} displayed ISV growth that was indistinguishable from wild-type siblings (Figures 2A, 2E, and 2F). Likewise, *flt4*^{um203} mutants did not exhibit ISV stalling as we previously described in morphants (Covassin et al., 2006), despite the presence of fully penetrant lymphatic defects (Figure 1B). We noted similar defects in an extracellular domain truncation allele as well (Table S2; data not shown), and *flt4*^{um203} mutants displayed significantly reduced transcript levels consistent with NMD (Figure 1B), similar to *fmnl3*^{um150} (Figure 2G). RT-PCR analysis of genotypically verified heterozygous and *fmnl3*^{um150} mutant sibling embryos ruled out exon skipping and confirmed that residual mRNA transcripts bore the mutant lesion (Figures 2H and 2I). Likewise, *pdgfrb* transcript was reduced in *pdgfrb*^{um148} mutant embryos and western blot analysis confirmed the absence of protein (Figures 2J and 2K).

Embryos bearing mutations in *amot*, *elmo1*, and *ets1* also displayed normal vascular patterning and circulatory function despite previous reports of defects in respective morphant embryos (Table S3; data not shown; Aase et al., 2007; Epting et al., 2010; Pham et al., 2007). In the case of the *ets1*^{um206} mutation, we detected transcripts missing exon 3, which contains the *um206* deletion, in heterozygous and mutant embryos (Figures 2L and 2M), while all remaining sequenced full-length transcripts bore the *um206* deletion (data not shown). In *ets1*, exon 3 encodes the pointed domain, which is essential for transcriptional activation by upstream kinases, such as ERK1/2 (Seidel and Graves, 2002). Thus, it is possible that *ets1*^{um206} is a hypomorphic allele. We also found that embryos bearing a truncation mutation in *neuropilin1a* (*nrp1a*; Figure 3A), a Vegf coreceptor also implicated in ISV patterning by previous studies using MO-mediated knockdown (Lee et al., 2002; Martyn and Schulte-Merker, 2004), displayed normal vascular patterning and circulation in the trunk blood vessels (Figures 3B and 3C). We did not investigate whether *pik3cg* or *smox* mutant embryos exhibited previously described morphant defects in blood cell development (Tijssen et al., 2011; Yoo et al., 2010), although both appeared normal until 5 days postfertilization and *smox* mutant zebrafish were viable to adulthood (data not shown). Thus, for seven of the candidate genes previously implicated in ISV sprouting using MO knockdown (*amot*, *elmo1*, *ets1*, *flt4*,

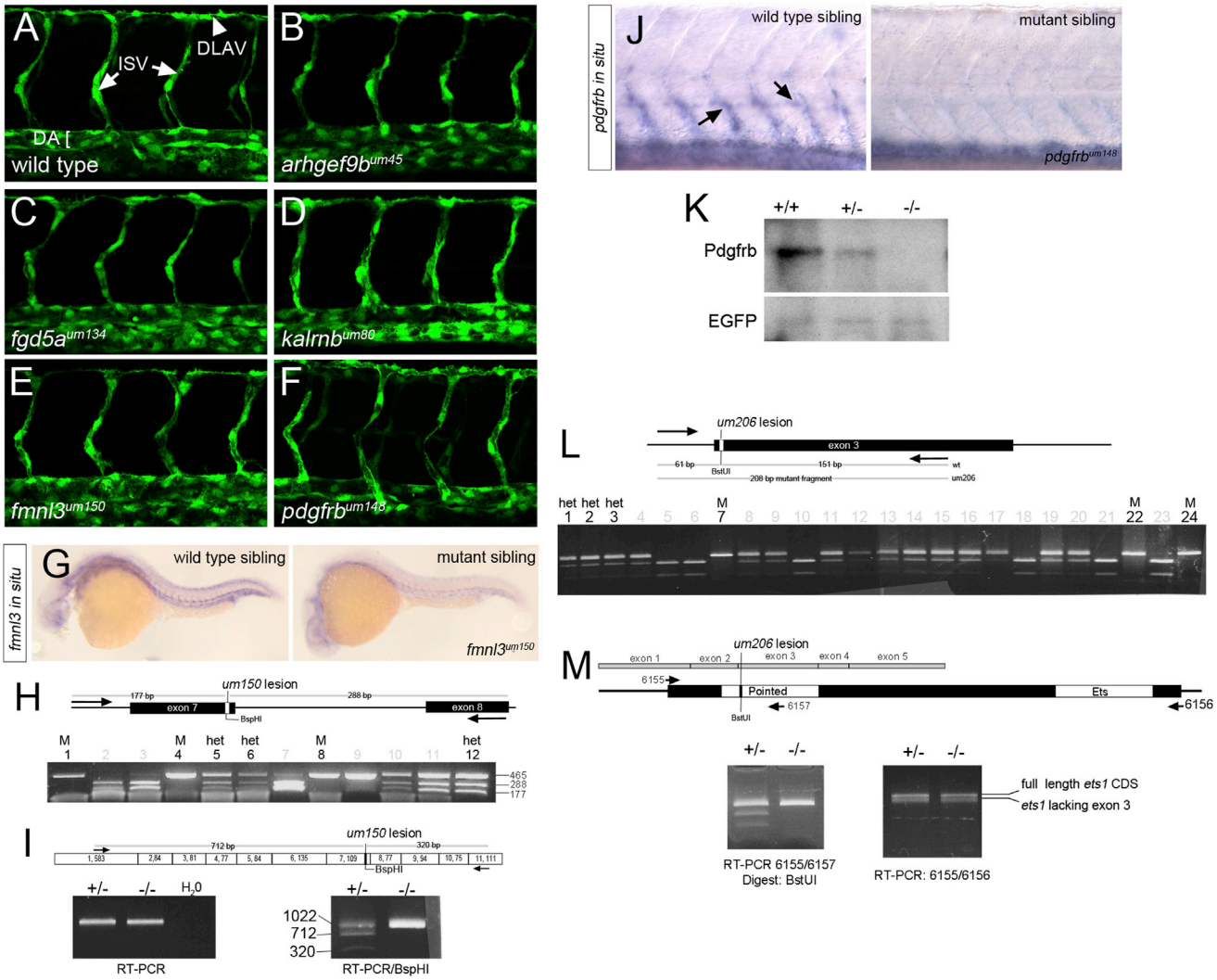

Figure 2. Normal ISV Development in Selected Mutant Embryos

(A–F) Confocal micrographs of *Tg(fli1a:egfp)*^{y1} or *Tg(kdrl:egfp)*^{s843} transgenic embryos at 32 hrpf subjected to immunostaining with GFP antibody. (A) Wild-type sibling: ISVs, DLAV, and DA are indicated. (B–F) Embryos mutant for (B) *arhgef9b*^{um45}, (C) *fgd5a*^{um134}, (D) *kalrnb*^{um80}, (E) *fmnl3*^{um150}, or (F) *pdgfrb*^{um148}. Lateral views, anterior to the left, and dorsal is up.

(G) Whole mount in situ hybridization analysis of *fmnl3* wild-type and *fmnl3*^{um150} mutant sibling at 26 hrpf. Lateral views, anterior to the left, and dorsal is up.

(H) Schematic of *fmnl3* locus flanking *um150* allele and genotyping of individual embryo heads at 72 hrpf from an in-cross of *fmnl3*^{um150} heterozygous carriers. Homozygous mutants and heterozygotes pooled for subsequent RT-PCR are indicated by M and het, respectively.

(I) Schematic of *fmnl3* transcript flanking *um150* and RT-PCR analysis of trunks from pooled M and het embryos shown in (H).

(J) Whole mount in situ hybridization analysis of *pdgfrb* in wild-type and *pdgfrb*^{um148} mutant at 72 hrpf. Lateral views, anterior to the left, and dorsal is up.

(K) Western blot analysis of Pdgfrb and Egfp in lysates from *Tg(fli1a:egfp)*^{y1};*pdgfrb*^{um148} of indicated genotype at 72 hrpf.

(L) Schematic of *ets1* exon 3 bearing the *um206* lesion and genotyping of individual embryo heads at 3 days postfertilization from an in-cross of *ets1*^{um206} heterozygous carriers.

(M) Schematic of *ets1* transcript and RT-PCR analysis of trunks from pooled M and het embryos shown in (L).

fmnl3, *nrp1a*, and *pdgfrb*), we failed to detect these defects in corresponding mutant embryos.

The discrepancies between morphant and mutant phenotypes may suggest that ISV sprouting is particularly sensitive to MO off-target effects. Therefore, we observed embryos bearing mutations in genes implicated in other aspects of development. Previous studies using MO-targeting have reported that *matrix metalloproteinase 2* (*mmp2*) is required for development of the primitive lymphatic system in zebrafish (Detry et al., 2012). We generated an allele (*mmp2*^{hu10535}) that produced a frameshift in the signal peptide and truncated the Mmp2 coding sequence (Figure 3D); a similar truncation in the signal peptide of *ccbe1* recapitulated lymphatic defects associated with previously described *ccbe1* alleles (Figure 1; Hogan et al., 2009a). By 5 days postfertilization, zebrafish larvae normally display formation of the TD and intersegmental lymphatic vessels (ISLVs), labeled in this case by a *flt4:mCitrine* transgene, lying adjacent to intersegmental arteries expressing

Table 1. Inconsistencies between Morphant and Mutant Phenotypes

	Morphant			Mutant	
Gene	Phenotype	Rescue	Reference	Zygotic Phenotype	Source
Morphants with Specific Phenotypes					
flt4	loss of lymphatics, stalled ISVs	ND	(Covassin et al., 2006)	loss of lymphatics	um
ccbe1	loss of lymphatics	ND	(Hogan et al., 2009a)	loss of lymphatics	hu
gata2a	lack of trunk circulation at 48 hrpf	ND	(Fiedler et al., 2011)	lack of trunk circulation	um
amot	stalled ISVs	yes	(Aase et al., 2007)	normal	um
elmo1	stalled ISVs	yes	(Epting et al., 2010)	normal	um
ets1	stalled ISVs, no circulation at 48 hrpf	ND	(Pham et al., 2007)	normal	um
fmnl3	stalled ISVs	yes	(Hetheridge et al., 2012)	normal	um
mmp2	loss of lymphatics	ND	(Detry et al., 2012)	normal	hu
nrp1a	ISV stalling and mispatterning	ND	(Martyn and Schulte-Merker, 2004)	normal[a]	hu
pdgfrb	ISV stalling	yes	(Wiens et al., 2010)	normal	hu
Morphants with Overt Phenotypes					
bmp7a	dorsalized	ND	(Lele et al., 2001)	dorsalized	sa
ttna	decreased heartbeat, edema	ND	(Seeley et al., 2007)	loss of heartbeat	sa
dag1	dystrophic	ND	(Parsons et al., 2002a)	dystrophic[a]	sa
lamc1	decreased length	ND	(Parsons et al., 2002b)	decreased length[a]	sa
tll1	dorsalized, loss of tail fin	ND	(Lele et al., 2001)	dorsalized, loss of tail fin[a]	sa
fam38a	gastrulation defective, fin blistering	ND	(Eisenhoffer et al., 2012)	normal	um
linc:birc6	hindbrain ventricle inflation	yes	(Ulitsky et al., 2011)	normal	um
appl1	necrosis, short yolk extension	yes	(Schenck et al., 2008)	normal[a]	sa
arrb1	severe delay and necrosis	yes	(Yue et al., 2009)	normal	sa
bmper	severe trunk malformation	ND	(Moser et al., 2007)	normal	sa
ccdc78	curved and shortened trunk	ND	(Majczenko et al., 2012)	normal	sa
cep290	cystic and slight curvature	ND	(Sayer et al., 2006)	normal	sa
col2a1a	curved trunk	ND	(Mangos et al., 2010)	normal	sa
hsp90ab1	shortened axis	ND	(Pei et al., 2007)	normal[a]	sa
glcci1	curved trunk	yes	(Nishibori et al., 2011)	normal	sa
hspg2	curved and shortened trunk	yes	(Zoeller et al., 2008)	normal	sa
htra1a	dorsalized	ND	(Kim et al., 2012a)	normal	sa
lratb	shortened and necrotic	yes	(Isken et al., 2007)	normal[a]	sa
itga2b	curved trunk	ND	(San Antonio et al., 2009)	normal	sa
nrp1a	curved trunk	ND	(Hillman et al., 2011)	normal[a]	sa
pcm1	curved, cystic	yes	(Stowe et al., 2012)	normal[a]	sa
mfn2	hindbrain ventricle inflation, curved trunk	yes	(Vettori et al., 2011)	normal	sa
ptenb	kinked trunk/tail	ND	(Croushore et al., 2005)	normal	sa
ptger4a	shortened axis	yes	(Cha et al., 2006)	normal	sa
usp33	CNS necrosis, curved trunk	ND	(Tse et al., 2009)	normal[a]	sa
zbtb4	dorsalized	yes	(Yao et al., 2010)	normal[a]	sa

ND, not determined; um, UMass Medical School; hu, Hubrecht Institute; and sa, Sanger ZMP.
[a]Possible maternal contribution.

flt1:tdTomato (Figure 3E). In embryos mutant for *mmp2*^{hu10535}, we similarly observed normal TD and ISLV development at this stage (Figure 3F). These results are in conflict with previous observations in morphant embryos (Detry et al., 2012) and suggest that *mmp2* may be dispensable for early lymphatic development in zebrafish.

Two of the mutant lines we generated were expected to display nonvascular phenotypes based on published morphant

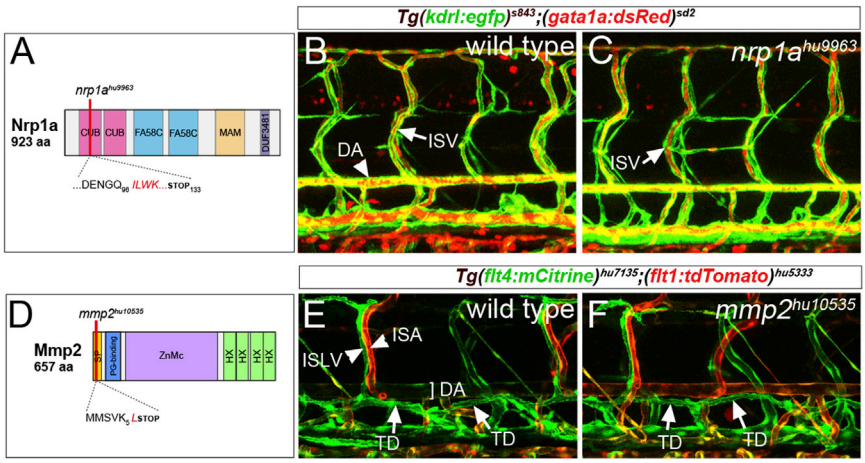

Figure 3. Normal Vascular and Lymphatic Development in *nrp1a* and *mmp2* Mutant Embryos

(A) Schematic of Nrp1a domain structure, indicating position of *nrp1a*^{hu9963}. CUB, CUB domain; FA58C, coagulation factor 5/8 C-terminal domain; MAM, MAM domain; and DUF3481, domain of unknown function.

(B and C) Confocal micrograph of embryos bearing Tg(*kdrl:egfp*)^{s843} (green) and *Tg*(*gata1a:dsRed*)^{sd2} (red) transgenes at 5 days post-fertilization. (B) Wild-type: DA and ISV are indicated. (C) *nrp1a*^{hu9963} mutant: ISV carrying red blood cells is indicated.

(D) Schematic of the Mmp2 and *mmp2*^{hu10535} allele. SP, signal peptide; PG-binding, peptidoglycan-binding domain; ZnMc, zinc-dependent metalloprotease; and HX, hemopexin-like repeats.

(E and F) Confocal micrographs of embryos bearing Tg(*flt4:mCitrine*)^{hu7135} (green) and *Tg*(*flt1:tdTomato*)^{hu5333} (red) transgenes. (E) Wild-type: ISLV, intersegmental artery (ISA), DA, and TD are indicated. (F) *mmp2*^{hu10535} mutant embryo.

data. In zebrafish, *fam38a* encodes the homolog of Piezo1, a multipass transmembrane protein that functions as a mechanosensory channel (Coste et al., 2012; Kim et al., 2012b). Knockdown of *fam38a* using a start codon MO causes early severe morphological defects, leading to speculation that maternal contribution is important for early development (Eisenhoffer et al., 2012). Inducible knockdown at later stages using a caged MO leads to epidermal masses in the developing fin fold due to defects in cell extrusion (Eisenhoffer et al., 2012). However, separate studies using both translational and splice-targeting MOs reported specific defects in red blood cell volume, similar to human patients bearing gain-of-function mutations in *PIEZO1* (Faucherre et al., 2014), but no overt defects. The *fam38a*^{um136} mutant is a frameshift leading to truncation of the Fam38a coding sequence (Figure 4A; Table S2). Consistent with NMD, we observed that *fam38a* transcript was reduced in *fam38a*^{um136} mutant embryos compared to wild-type siblings (Figures 4B and 4C). RT-PCR analysis of residual *fam38a* transcript from mutant embryos did not reveal exon skipping or presence of wild-type transcripts (Figures 4D–4F). Interestingly, we noted a low frequency of deletions larger than the *um136* lesion, suggesting that this microdeletion affects splicing, although all deletions in the transcript resulted in a frameshift (Figure 4G). Despite the presence of this mutation, fin morphology was indistinguishable between wild-type and *fam38a*^{um136} mutant sibling embryos at 72 hrpf (Figures 5H and 5I). Together with the discrepancies between published reports utilizing a translation-blocking MO, these results suggest that the overt gastrulation and fin defects from previous studies (Eisenhoffer et al., 2012) may have been due to off-target effects.

The mutants described above bear frameshifts and, in selected cases, we observed evidence of NMD or loss of protein. However, we also noted exon skipping and possible effects on splicing. A more desirable strategy to generate a null allele would be to introduce a large deletion in a locus of interest. This approach would be particularly useful for deleting noncoding RNAs for which functional domains are difficult to identify. We have previously applied two pairs of TALENs targeting adjacent *cis* sequences to delete the locus encoding the long noncoding RNA *linc:birc6*, also referred to as *megamind* (Gupta et al., 2013; Ulitsky et al., 2011). MO-mediated knockdown of *megamind* in zebrafish caused hydrocephaly, as indicated by inflation of hindbrain ventricles (Ulitsky et al., 2011). We established a zebrafish line (*megamind*^{um209}) bearing a segmental deletion that eliminated transcripts arising from the *megamind* locus, but that did not affect the *cyrano* lncRNA or expression of *eef1a1l1* mRNA (Figures 5A and 5B). Despite the absence of *megamind* RNA in mutant embryos, they were morphologically indistinguishable from wild-type (Figures 5C and 5D). The *megamind*^{um209} mutants were viable into adulthood and embryos derived from in-crosses of *megamind*^{um209} homozygous adults were normal (Figure 5D). Similar results were observed for a second independent deletion of the *megamind* locus (Table S2; data not shown). The deletion in *megamind*^{um209} mutant embryos also removed the sequences targeted by published MOs (Figure 5A; Ulitsky et al., 2011). Strikingly, injection of a previously described MO targeting *megamind* induced the appearance of inflated hindbrain ventricles in both wild-type siblings and *megamind*^{um209} mutant embryos, despite the absence of the MO target site in the latter (Figures 5E and 5F). In this case, the MO target sequence bore only modest homology to other *megamind* paralogs within the genome (68% and 76%). We would point out that similar phenotypes were observed with splice site MOs that would not be expected to target these other long noncoding RNAs (Ulitsky et al., 2011). The MO would also not be expected to reduce expression of the related *tuna* long noncoding RNA that recently has been implicated in brain development in zebrafish (Lin et al., 2014). Thus, these observations suggest that the previously reported *megamind* phenotype is likely due to MO off-target effects.

Evidence of a High False-Positive Rate for Morphant Phenotypes

Our results suggest that many morphant phenotypes are not recapitulated in mutant embryos. To assess how universal this

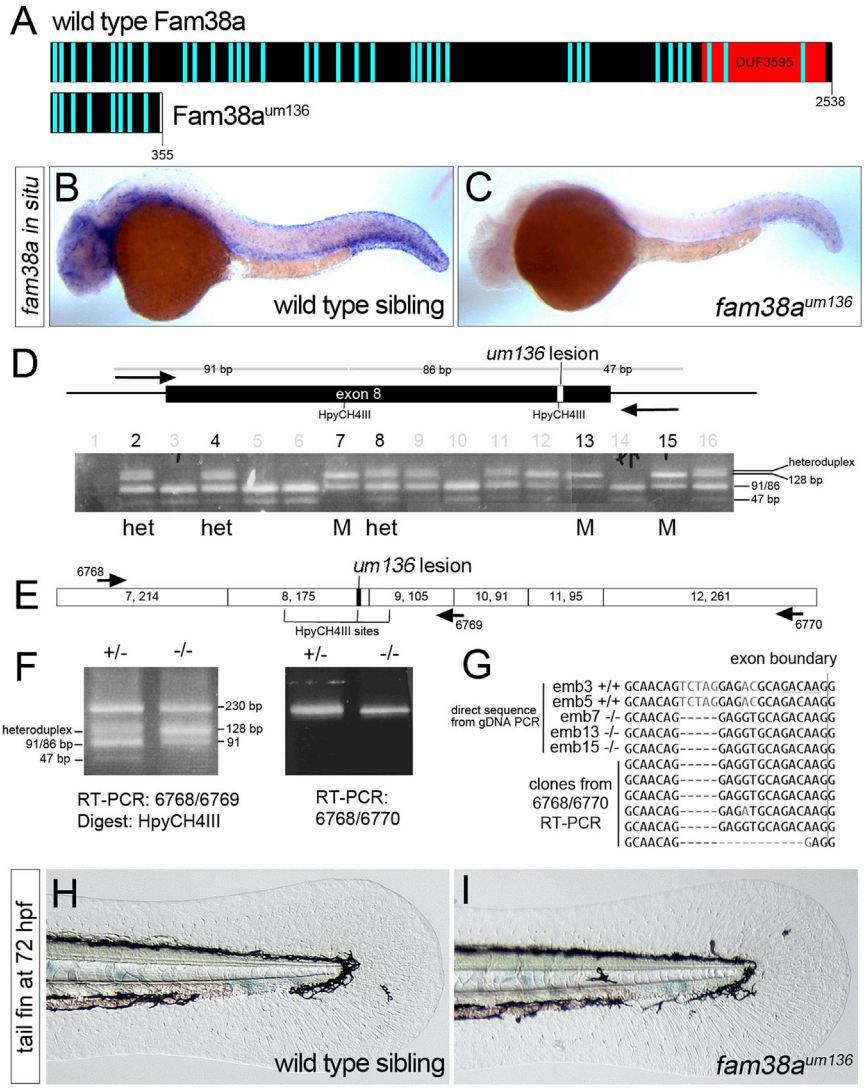

Figure 4. Normal Fin Development in *fam38a* Mutant Embryos

(A) Schematic of Fam38a and truncated Fam38a^{um136}. Light blue bars, transmembrane domains; DUF, domain of unknown function.

(B and C) Whole mount in situ hybridization of *fam38a* in (B) wild-type and (C) *fam38a*^{um136} mutant at 28 hrpf.

(D) Schematic of *fam38a* exon 8 with *um136* lesion and genotyping of individual embryo heads at 72 hrpf from an in-cross of *fam38a*^{um136} heterozygous carriers. Homozygous mutants and heterozygotes pooled for subsequent RT-PCR are indicated by M and het, respectively.

(E) Schematic of exons in *fam38a* transcript (numbers in each box indicate exon number, followed by exon size).

(F) RT-PCR analysis of *fam38a* transcript in heterozygous and *fam38a*^{um136} mutant trunks pooled from the het and M embryos in (D).

(G) Top five sequences are directly from PCR products from genomic DNA of numbered individuals in (D). HpyCH4III site is underlined and the 5-bp *um136* deletion is evident. Bottom six sequences are cloned fragments from RT-PCR of pooled *fam38a*^{um136} mutant embryos (embryos 7, 13, and 15).

(H and I) Transmitted light images of the tail fin fold in live (H) wild-type and (I) *fam38a*^{um136} mutant embryos at 72 hrpf.

finding might be, we performed an integrative analysis of curated data sets available from ZFIN and the Sanger ZMP, which has reported phenotypic analysis of mutant embryos for more than 700 genes (Kettleborough et al., 2013). We identified 98 ZMP mutants for which morphant phenotypes have been published. We restricted analysis to overt morphant phenotypes that affected the whole embryo and would have been seen easily in the ZMP phenotyping pipeline. We further performed literature-based validation of ZFIN data and eliminated any ZMP mutants unlikely to affect protein function (Table S4) to yield 24 genes for comparison (Table S5). Mutations in only five of these genes resulted in observable phenotypes that were largely consistent with MO knockdown experiments, while the rest did not (Figure 6; Table 1; Table S5). We did not note any obvious pattern in effective dosage, rescue penetrance, p53 rescue, or other variable that predicted whether a MO would yield a discordant phenotype (Tables S3 and S5).

The discrepancies between morphants and mutants may be due to the use of a MO targeting the start codon, which blocks translation of maternal mRNAs, while mutant embryos derived from heterozygotes lack only zygotic gene function. Therefore, we took into account two additional data sets: (1) nature of MO target sequence (translation, which would block maternal transcript translation, versus splice-blocking, which would affect only zygotic transcripts) used in each published study; and (2) available RNA-Seq data (Harvey et al., 2013) to assess candidate mRNA levels at the two-cell stage. We also considered studies in which maternal effects had been ruled out in published studies (e.g., *ptenb*; Faucherre et al., 2008), as well as transcript analysis and crosses of homozygous mutants in our own lines (see above; Table S3). After applying these restrictions, we identified 14 ZMP mutants and 12 in our collection where maternal contribution was unlikely (Tables S3 and S5; *flt4* was counted twice as it recapitulates lymphatic but not ISV defects). In these cases, 12 of 14 Sanger mutants and 9 of 12 of our mutants failed to exhibit published morphant phenotypes (Tables S3 and S5; Figure 6). Thus, even when considering the maternal contribution, more than 70% of morphant phenotypes were not observed in respective mutants from two separate collections (Figure 6).

DISCUSSION

The development of programmable site-specific nucleases for genome modification now enables reverse genetic approaches to be applied in model and nonmodel organisms. As an initial step to broadly apply these tools in zebrafish, we have used

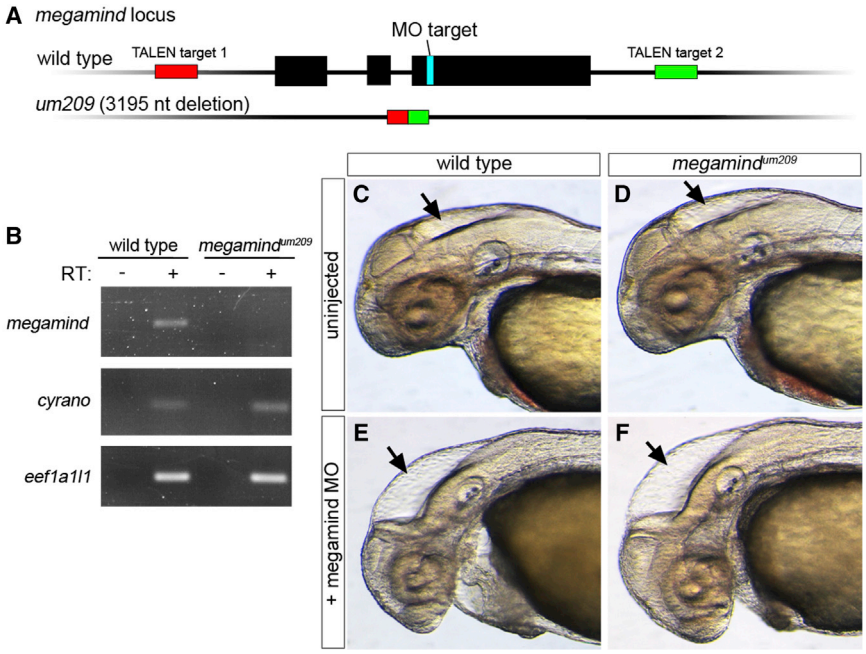

Figure 5. Normal Hindbrain Development in *megamind* Mutant Embryos

(A) Schematic of the *megamind* locus in wild-type and *megamind*^{um209} mutants. The red and green boxes indicate relative position of the TALEN target sequences, and the MO target sequence is shown.

(B) RT-PCR for the *megamind* and *cyrano* lincRNAs as well as *eef1a1l1* in wild-type and *megamind*^{um209} mutant embryos. RT refers to RNA template without (−) or with (+) reverse transcription.

(C–F) Transmitted light images of the head region in embryos at 48 hrpf. The hindbrain ventricle is indicated with an arrow in each image. Lateral views, anterior to the left, and dorsal is up. (C) Wild-type, uninjected; (D) *megamind*^{um209} mutant; (E) wild-type injected with 20 ng *megamind* conserved site MO; and (F) *megamind*^{um209} mutant injected with *megamind* conserved site MO.

ZFNs, TALENs, and the clustered, regularly interspaced, short palindromic repeats (CRISPR) system to generate a collection of lines bearing mutations in candidate genes of interest. Despite the expression of most of our candidate genes in endothelial cells at early embryonic stages of development and their homology to known functional molecules, we failed to observe any notable vascular defects in mutant embryos for most of the genes analyzed. In this regard, our findings are consistent with low rates of overt phenotypes in a recent characterization of nearly 1,000 zebrafish mutant lines (Kettleborough et al., 2013) and suggest a high degree of redundancy is built into the zebrafish genome.

A more troubling finding from our work is the discrepancy between morphant and mutant phenotypes. Our integrative analysis of ZMP and ZFIN data sets showed a high rate of discrepancy even when taking into account maternal contribution. A caveat here is that we restricted analysis to overt phenotypes that were also the most likely phenotypes to have been caused by MO off-target effects. Also, some ZMP point mutants may not be null alleles. Thus, the true false-positive rate may not be as high when considering more specific defects in null mutants. However, in our mutants, which mostly bore deletions resulting in frameshifts, we focused on subtle vascular defects in a sensitive transgenic background. We also observed evidence of NMD or loss of protein in selected mutants, supporting the fact that many are likely null alleles, yet we still observed a high false-positive morphant phenotype rate. Consistent with these observations, recent studies have reported inconsistencies between morphants and mutants for individual genes, including phenotypes affecting lymphatic development (for *nr2f2,* Aranguren et al., 2011; Swift et al., 2014; van Impel et al., 2014), neuronal function (for *mfn2* and *prp2*, Chapman et al., 2013; Fleisch et al., 2013; Nourizadeh-Lillabadi et al., 2010; Vettori et al., 2011), hindbrain patterning (for *gbx2*, Kikuta et al., 2003; Su et al., 2014), and lateral line development (for *tcf7*, Aman et al., 2011). Taken together with our broader findings here, these studies raise a major concern about relying solely on the application of MOs for primary characterization of gene function in the zebrafish.

Our results suggest that many morphant phenotypes may be due to off-target effects. The most striking is the *megamind* mutant, where we recapitulated the morphant phenotype in embryos lacking the MO target site. This is especially worrisome as *megamind* morphants could be rescued by coinjecting *megamind* RNA (Ulitsky et al., 2011). Likewise, 5 of 12 of the morphant phenotypes that we failed to observe in mutants were rescued in previous studies (Table S3). Similar observations recently have been made for zebrafish *pak4*, which is genetically dispensable for development, despite a morphant phenotype that can be rescued by mRNA injection (Law and Sargent, 2014). Given the high copy number of injected MO (10 ng of a MO is equal to approximately 6.3×10^{11} molecules) as well as the rescue RNA, which is typically coinjected, it is possible that nonspecific interference of the coinjected RNA with the MO may lead to reduced knockdown efficiency and apparent rescue. Most studies also fail to confirm that endogenous protein or transcript is similarly affected by MO injection in both the absence and presence of rescue mRNA. Thus, current methods of rescue for morphant phenotypes are not a reliable guideline for verification of MO specificity.

MO off-target effects have been attributed to p53 induction that leads to apoptosis (Robu et al., 2007) and can cause seemingly specific gene expression changes in certain cell types (Amoyel et al., 2005; Gerety and Wilkinson, 2011). However, little is known concerning the mechanism by which MOs induce p53 activation. While characteristics of the MO backbone are thought to reduce interactions with macromolecules, there are only anecdotal claims to this effect (Summerton, 2007) and no studies have investigated off-target effects independent of RNA binding. Furthermore, MOs bearing up to four base mismatches can effectively inhibit target mRNA, suggesting a

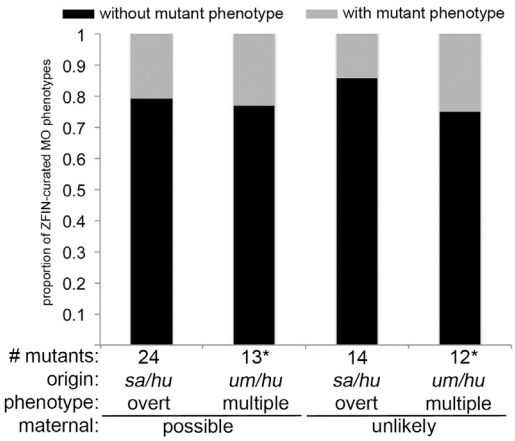

Figure 6. Results of Integrative Analysis of Sanger Center and ZFIN-Curated Mutant and Morphant Data Sets

Graph shows proportion of all genes with associated morphant phenotypes that display or do not display a corresponding mutant phenotype. **flt4* is included in both categories (with and without mutant phenotype) as lymphatic defects match the mutant, while ISV defects do not. Allele designations: hu, Hubrecht Institute; sa, Sanger Center; um, UMass Medical School.

wide spectrum of off-target RNA binding. Thus, more global effects on translation, splicing, and, possibly, small RNA processing are possible. This, in turn, could trigger the induction of p53. In this case, p53 knockdown would only ameliorate some of the observed off-target effects. Notably, a recent study demonstrated that a morphant phenotype not rescued by p53 knockdown, and, therefore, thought to be specifically caused by knockdown of the target gene, also was not seen in the corresponding null maternal/zygotic mutant (Law and Sargent, 2014). Thus, similar to mRNA injection, p53 knockdown may not be a reliable indicator for the specificity of a morphant phenotype. If MOs are to be applied as a tool in parallel with targeted gene knockout to discern gene function, further studies are needed to clarify the mechanism of off-target responses.

The ability to knock down candidate genes of interest using MOs clearly had an impactful role in the application of the zebrafish as a model system. Indeed, nearly 300 morphant phenotypes curated in ZFIN are consistent with those observed in mutant embryos (unpublished data), as were several in this study. However, there have long been anecdotal claims within the zebrafish-studying community of problematic p53-independent off-target effects and variability due to different preparations of the same MO. Based on these reports, Drs. Judith Eisen and James Smith (Eisen and Smith, 2008) published a list of guidelines for the reliable application of MOs in frog and zebrafish. Among their recommendations was that, whenever possible, investigators confirm a morphant phenotype by comparison to a mutant, if available. Our findings here suggest that this is the most essential guideline to follow. At the same time, it is also important to validate the characteristics of newly generated mutant lines in parallel to confirm their effect on candidate gene function. Indeed, we noted cases of exon skipping and splicing defects in some mutants. Moving forward, we recommend targeting exons encoding domains that are necessary for protein function or generating segmental deletions. Given the ease of use of current site-specific nuclease technologies, most notably the CRISPR systems, we would advocate for widespread application of these approaches to generate mutants. While this approach requires a significant research investment (typically between 6 and 12 months from initial injections to phenotypic characterization of mutant phenotypes), our observations demonstrate the need for a genetic approach as the definitive determination of gene function. Moreover, we would suggest broader community-wide and editorial guidelines that require an observed MO-induced phenotype to be validated in embryos bearing mutations in the same gene, after which a MO could then be reliably applied for subsequent functional studies.

EXPERIMENTAL PROCEDURES

Zebrafish Handling and Maintenance

Zebrafish were maintained in accordance with approved institutional protocols at the University of Massachusetts Medical School and the Hubrecht Institute. The *Tg(fli1a:egfp)^{y1}*, *Tg(kdrl:egfp)^{s843}*, *Tg(gata1a:dsRed)^{sd2}*, *Tg(flt4:mCitrine)^{hu7135}*, and *Tg(flt1:tdTomato)^{hu5333}* transgenic lines have been described elsewhere (Beis et al., 2005; Bussmann et al., 2010; Lawson and Weinstein, 2002; Traver et al., 2003; van Impel et al., 2014).

Construction of Site-Specific Nucleases

ZFNs or TALENs were constructed as described elsewhere (Kok et al., 2014). Appropriate zinc finger cassettes and target sites were identified in candidate genes using previously described databases of targets identified in the zebrafish genome (Gupta et al., 2012; Zhu et al., 2011). TALEN sequences were identified in candidate genes using TAL Effector Nucleotide Targeter 2.0 (https://tale-nt.cac.cornell.edu/). The list of target sites within candidate genes can be found in Table S2. All nuclease sequences are available upon request. Generation of mutant lines was performed as described elsewhere (Kok et al., 2014; Meng et al., 2008; Gupta et al., 2013). A sgRNA targeting *ets1* (Table S2) was chosen based on location in a functional domain and presence of restriction enzyme site useful for genotyping. The sgRNA was synthesized and used to generate mutant founders based on published protocols (Gagnon et al., 2014).

Phenotypic Analysis

Embryos derived from identified heterozygous carriers were observed every day for the first 5 days of development using a dissection microscope. Transmitted light and differential interference contrast images as well as analysis of vascular or lymphatic morphology using confocal or two-photon microscopy were performed as described elsewhere (Quillien et al., 2014; van Impel et al., 2014). In some cases, transgenic embryos were fixed and subjected to immunostaining with GFP antibody to boost the fluorescent signal, as we have done previously (Covassin et al., 2006). All embryos were subsequently subjected to individual genotypic analysis, which was performed using restriction digest of PCR fragments encompassing the targeted sequence, as we have done previously (Meng et al., 2008).

RT-PCR and Western Blot Analysis

We performed RT-PCR or western blot analysis on wild-type and mutant sibling embryos. Individual embryos were anesthetized according to standard protocols; their heads were removed using a scalpel and each was transferred to an individual well of a 96-well plate. In parallel, the trunk region was transferred to individual Eppendorf tubes in a dry ice/ethanol bath and subsequently stored at −80°C. Embryo heads were used for genomic DNA isolation and genotype analysis, as described previously (Meng et al., 2008). Several trunks of genotypically identical embryos were pooled and dissociated in Trizol, or lysed in sample buffer for protein isolation. Reverse transcription of total RNA was performed using oligo-dT and Superscript III (Invitrogen) according to the manufacturer's protocols. PCR was performed using primers listed in the Supplemental Experimental Procedures. PCR fragments from genomic DNA were directly sequenced, while those from cDNA were cloned into pGEM-T (Promega) prior to sequencing. Western blot analysis was performed according to standard protocols. An antibody against zebrafish Pdgfrb was raised in rabbits (Innovagen) using a synthetic peptide (KYADIQPSPYESPYQQDIYQ).

Riboprobes

Fragments for synthesizing riboprobes were amplified from wild-type cDNA and cloned into pGEM-T by TA cloning (Promega). Oligonucleotide primers are listed in the Supplemental Experimental Procedures. To generate digoxigenin-labeled antisense riboprobes, DNA templates were first generated from plasmids using M13 forward and reverse primers. Templates were purified by ethanol precipitation and used for in vitro transcription using the appropriate bacteriophage RNA polymerase. The riboprobe against *pdgfrb* was prepared by linearizing the template plasmid with Apa I prior to synthesis with RNA polymerase.

Integration of Sanger and ZFIN Data Sets

We downloaded the list of phenotyped mutants generated through the Sanger ZMP resource from the Sanger Center website (http://www.sanger.ac.uk/sanger/Zebrafish_Zmpbrowse). We downloaded and extracted all morphant data from the ZFIN (http://zfin.org/downloads/phenoGeneCleanData.txt). Both downloads were done in April 2014. Data sets were crossreferenced to identify genes for which MO-mediated knockdown resulted in a phenotype and a corresponding mutant had been subjected to phenotypic analysis (98 genes). We next restricted analysis to only whole-embryo phenotypes, (Field = "_Affected_structure_or_Process_1_superterm_Name," term = "whole organism"), yielding 33 genes. This list was subsequently annotated manually through primary literatures searches to confirm that curated ZFIN data were accurate. From this analysis, we eliminated four genes that gave subtle morphant phenotypes and one gene that did not recapitulate the phenotype of a previously existing mutant. We further removed four genes that were less likely to bear severely mutagenic alleles (Table S4). To assess maternal contribution, we integrated published RNA-Seq data (Harvey et al., 2013) and verified application of translation or splice blocking MOs from the primary literature in each case. We also took into account other published sources investigating genetic maternal requirement, including our observations in this study. Genes for which fragments per kilobase per million (FPKM) was 0, or that displayed a phenotype with a splice-blocking MO, were classified as unlikely to contribute maternal function. All others were classified as possible.

SUPPLEMENTAL INFORMATION

Supplemental Information includes Supplemental Experimental Procedures, one figure, and five tables and can be found with this article online at http://dx.doi.org/10.1016/j.devcel.2014.11.018.

AUTHOR CONTRIBUTIONS

F.O.K., M.S., C-W.N., A.G., A.v.I., B.C.K., and J.P.-M. generated mutant lines and performed phenotypic analysis. A.S.G. and L.E. contributed to molecular and phenotypic characterization of the *pdgfrb* line. L.E. and C.B. provided the Pdgfrb antibody. G.K., I.M., and D.F.D. provided essential technical support, including identification of carrier fish and genotyping of embryos. S.S.T. provided support in the identification of candidate endothelial genes. N.D.L. generated the *ets1* mutant, performed molecular analyses on mutants, and wrote the paper. S.S.-M. and S.A.W., along with all the authors, contributed to the preparation and editing of the manuscript.

ACKNOWLEDGMENTS

This work was funded by grants to N.D.L. (R01HL079266, R01HL101374) and a multi-investigator grant to N.D.L. and S.A.W. (R01HL093766) from the National Heart, Lung, and Blood Institute. S.S.-M. was supported by the Deutsche Forschungsgemeinschaft (DFG), Cells-in-Motion Cluster of Excellence (EXC 1003-CiM), University of Münster, Germany.

Received: June 1, 2014
Revised: August 19, 2014
Accepted: November 10, 2014
Published: December 18, 2014

REFERENCES

Aase, K., Ernkvist, M., Ebarasi, L., Jakobsson, L., Majumdar, A., Yi, C., Birot, O., Ming, Y., Kvanta, A., Edholm, D., et al. (2007). Angiomotin regulates endothelial cell migration during embryonic angiogenesis. Genes Dev. *21*, 2055–2068.

Aman, A., Nguyen, M., and Piotrowski, T. (2011). Wnt/β-catenin dependent cell proliferation underlies segmented lateral line morphogenesis. Dev. Biol. *349*, 470–482.

Amoyel, M., Cheng, Y.C., Jiang, Y.J., and Wilkinson, D.G. (2005). Wnt1 regulates neurogenesis and mediates lateral inhibition of boundary cell specification in the zebrafish hindbrain. Development *132*, 775–785.

Aranguren, X.L., Beerens, M., Vandevelde, W., Dewerchin, M., Carmeliet, P., and Luttun, A. (2011). Transcription factor COUP-TFII is indispensable for venous and lymphatic development in zebrafish and Xenopus laevis. Biochem. Biophys. Res. Commun. *410*, 121–126.

Bedell, V.M., Wang, Y., Campbell, J.M., Poshusta, T.L., Starker, C.G., Krug, R.G., 2nd, Tan, W., Penheiter, S.G., Ma, A.C., Leung, A.Y., et al. (2012). In vivo genome editing using a high-efficiency TALEN system. Nature *491*, 114–118.

Beis, D., Bartman, T., Jin, S.W., Scott, I.C., D'Amico, L.A., Ober, E.A., Verkade, H., Frantsve, J., Field, H.A., Wehman, A., et al. (2005). Genetic and cellular analyses of zebrafish atrioventricular cushion and valve development. Development *132*, 4193–4204.

Bussmann, J., Bos, F.L., Urasaki, A., Kawakami, K., Duckers, H.J., and Schulte-Merker, S. (2010). Arteries provide essential guidance cues for lymphatic endothelial cells in the zebrafish trunk. Development *137*, 2653–2657.

Cade, L., Reyon, D., Hwang, W.Y., Tsai, S.Q., Patel, S., Khayter, C., Joung, J.K., Sander, J.D., Peterson, R.T., and Yeh, J.R. (2012). Highly efficient generation of heritable zebrafish gene mutations using homo- and heterodimeric TALENs. Nucleic Acids Res. *40*, 8001–8010.

Cha, Y.I., Kim, S.H., Sepich, D., Buchanan, F.G., Solnica-Krezel, L., and DuBois, R.N. (2006). Cyclooxygenase-1-derived PGE2 promotes cell motility via the G-protein-coupled EP4 receptor during vertebrate gastrulation. Genes Dev. *20*, 77–86.

Chapman, A.L., Bennett, E.J., Ramesh, T.M., De Vos, K.J., and Grierson, A.J. (2013). Axonal Transport Defects in a Mitofusin 2 Loss of Function Model of Charcot-Marie-Tooth Disease in Zebrafish. PLoS ONE *8*, e67276.

Chen, S., Oikonomou, G., Chiu, C.N., Niles, B.J., Liu, J., Lee, D.A., Antoshechkin, I., and Prober, D.A. (2013). A large-scale in vivo analysis reveals that TALENs are significantly more mutagenic than ZFNs generated using context-dependent assembly. Nucleic Acids Res. *41*, 2769–2778.

Choi, W.Y., Giraldez, A.J., and Schier, A.F. (2007). Target protectors reveal dampening and balancing of Nodal agonist and antagonist by miR-430. Science *318*, 271–274.

Coste, B., Xiao, B., Santos, J.S., Syeda, R., Grandl, J., Spencer, K.S., Kim, S.E., Schmidt, M., Mathur, J., Dubin, A.E., et al. (2012). Piezo proteins are pore-forming subunits of mechanically activated channels. Nature *483*, 176–181.

Covassin, L.D., Villefranc, J.A., Kacergis, M.C., Weinstein, B.M., and Lawson, N.D. (2006). Distinct genetic interactions between multiple Vegf receptors are required for development of different blood vessel types in zebrafish. Proc. Natl. Acad. Sci. USA *103*, 6554–6559.

Covassin, L.D., Siekmann, A.F., Kacergis, M.C., Laver, E., Moore, J.C., Villefranc, J.A., Weinstein, B.M., and Lawson, N.D. (2009). A genetic screen for vascular mutants in zebrafish reveals dynamic roles for Vegf/Plcg1 signaling during artery development. Dev. Biol. *329*, 212–226.

Croushore, J.A., Blasiole, B., Riddle, R.C., Thisse, C., Thisse, B., Canfield, V.A., Robertson, G.P., Cheng, K.C., and Levenson, R. (2005). Ptena and ptenb genes play distinct roles in zebrafish embryogenesis. Dev. Dyn. *234*, 911–921.

Dahlem, T.J., Hoshijima, K., Jurynec, M.J., Gunther, D., Starker, C.G., Locke, A.S., Weis, A.M., Voytas, D.F., and Grunwald, D.J. (2012). Simple methods for generating and detecting locus-specific mutations induced with TALENs in the zebrafish genome. PLoS Genet. *8*, e1002861.

Detry, B., Erpicum, C., Paupert, J., Blacher, S., Maillard, C., Bruyère, F., Pendeville, H., Remacle, T., Lambert, V., Balsat, C., et al. (2012). Matrix

metalloproteinase-2 governs lymphatic vessel formation as an interstitial collagenase. Blood *119*, 5048–5056.

Doyon, Y., McCammon, J.M., Miller, J.C., Faraji, F., Ngo, C., Katibah, G.E., Amora, R., Hocking, T.D., Zhang, L., Rebar, E.J., et al. (2008). Heritable targeted gene disruption in zebrafish using designed zinc-finger nucleases. Nat. Biotechnol. *26*, 702–708.

Draper, B.W., Morcos, P.A., and Kimmel, C.B. (2001). Inhibition of zebrafish fgf8 pre-mRNA splicing with morpholino oligos: a quantifiable method for gene knockdown. Genesis *30*, 154–156.

Driever, W., Solnica-Krezel, L., Schier, A.F., Neuhauss, S.C., Malicki, J., Stemple, D.L., Stainier, D.Y., Zwartkruis, F., Abdelilah, S., Rangini, Z., et al. (1996). A genetic screen for mutations affecting embryogenesis in zebrafish. Development *123*, 37–46.

Eisen, J.S., and Smith, J.C. (2008). Controlling morpholino experiments: don't stop making antisense. Development *135*, 1735–1743.

Eisenhoffer, G.T., Loftus, P.D., Yoshigi, M., Otsuna, H., Chien, C.B., Morcos, P.A., and Rosenblatt, J. (2012). Crowding induces live cell extrusion to maintain homeostatic cell numbers in epithelia. Nature *484*, 546–549.

Ekker, S.C., and Larson, J.D. (2001). Morphant technology in model developmental systems. Genesis *30*, 89–93.

Epting, D., Wendik, B., Bennewitz, K., Dietz, C.T., Driever, W., and Kroll, J. (2010). The Rac1 regulator ELMO1 controls vascular morphogenesis in zebrafish. Circ. Res. *107*, 45–55.

Faucherre, A., Taylor, G.S., Overvoorde, J., Dixon, J.E., and Hertog, Jd. (2008). Zebrafish pten genes have overlapping and non-redundant functions in tumorigenesis and embryonic development. Oncogene *27*, 1079–1086.

Faucherre, A., Kissa, K., Nargeot, J., Mangoni, M.E., and Jopling, C. (2014). Piezo1 plays a role in erythrocyte volume homeostasis. Haematologica *99*, 70–75.

Fiedler, J., Jazbutyte, V., Kirchmaier, B.C., Gupta, S.K., Lorenzen, J., Hartmann, D., Galuppo, P., Kneitz, S., Pena, J.T., Sohn-Lee, C., et al. (2011). MicroRNA-24 regulates vascularity after myocardial infarction. Circulation *124*, 720–730.

Fleisch, V.C., Leighton, P.L., Wang, H., Pillay, L.M., Ritzel, R.G., Bhinder, G., Roy, B., Tierney, K.B., Ali, D.W., Waskiewicz, A.J., and Allison, W.T. (2013). Targeted mutation of the gene encoding prion protein in zebrafish reveals a conserved role in neuron excitability. Neurobiol. Dis. *55*, 11–25.

Gagnon, J.A., Valen, E., Thyme, S.B., Huang, P., Ahkmetova, L., Pauli, A., Montague, T.G., Zimmerman, S., Richter, C., and Schier, A.F. (2014). Efficient mutagenesis by Cas9 protein-mediated oligonucleotide insertion and large-scale assessment of single-guide RNAs. PLoS ONE *9*, e98186.

Gerety, S.S., and Wilkinson, D.G. (2011). Morpholino artifacts provide pitfalls and reveal a novel role for pro-apoptotic genes in hindbrain boundary development. Dev. Biol. *350*, 279–289.

Gupta, A., Christensen, R.G., Rayla, A.L., Lakshmanan, A., Stormo, G.D., and Wolfe, S.A. (2012). An optimized two-finger archive for ZFN-mediated gene targeting. Nat. Methods *9*, 588–590.

Gupta, A., Hall, V.L., Kok, F.O., Shin, M., McNulty, J.C., Lawson, N.D., and Wolfe, S.A. (2013). Targeted chromosomal deletions and inversions in zebrafish. Genome Res. *23*, 1008–1017.

Haffter, P., Granato, M., Brand, M., Mullins, M.C., Hammerschmidt, M., Kane, D.A., Odenthal, J., van Eeden, F.J., Jiang, Y.J., Heisenberg, C.P., et al. (1996). The identification of genes with unique and essential functions in the development of the zebrafish, Danio rerio. Development *123*, 1–36.

Hammerschmidt, M., Pelegri, F., Mullins, M.C., Kane, D.A., Brand, M., van Eeden, F.J., Furutani-Seiki, M., Granato, M., Haffter, P., Heisenberg, C.P., et al. (1996). Mutations affecting morphogenesis during gastrulation and tail formation in the zebrafish, Danio rerio. Development *123*, 143–151.

Harvey, S.A., Sealy, I., Kettleborough, R., Fenyes, F., White, R., Stemple, D., and Smith, J.C. (2013). Identification of the zebrafish maternal and paternal transcriptomes. Development *140*, 2703–2710.

Hetheridge, C., Scott, A.N., Swain, R.K., Copeland, J.W., Higgs, H.N., Bicknell, R., and Mellor, H. (2012). The formin FMNL3 is a cytoskeletal regulator of angiogenesis. J. Cell Sci. *125*, 1420–1428.

Hillman, R.T., Feng, B.Y., Ni, J., Woo, W.M., Milenkovic, L., Hayden Gephart, M.G., Teruel, M.N., Oro, A.E., Chen, J.K., and Scott, M.P. (2011). Neuropilins are positive regulators of Hedgehog signal transduction. Genes Dev. *25*, 2333–2346.

Hogan, B.M., Bos, F.L., Bussmann, J., Witte, M., Chi, N.C., Duckers, H.J., and Schulte-Merker, S. (2009a). Ccbe1 is required for embryonic lymphangiogenesis and venous sprouting. Nat. Genet. *41*, 396–398.

Hogan, B.M., Herpers, R., Witte, M., Heloterä, H., Alitalo, K., Duckers, H.J., and Schulte-Merker, S. (2009b). Vegfc/Flt4 signalling is suppressed by Dll4 in developing zebrafish intersegmental arteries. Development *136*, 4001–4009.

Hwang, W.Y., Fu, Y., Reyon, D., Maeder, M.L., Tsai, S.Q., Sander, J.D., Peterson, R.T., Yeh, J.R., and Joung, J.K. (2013). Efficient genome editing in zebrafish using a CRISPR-Cas system. Nat. Biotechnol. *31*, 227–229.

Isken, A., Holzschuh, J., Lampert, J.M., Fischer, L., Oberhauser, V., Palczewski, K., and von Lintig, J. (2007). Sequestration of retinyl esters is essential for retinoid signaling in the zebrafish embryo. J. Biol. Chem. *282*, 1144–1151.

Isogai, S., Lawson, N.D., Torrealday, S., Horiguchi, M., and Weinstein, B.M. (2003). Angiogenic network formation in the developing vertebrate trunk. Development *130*, 5281–5290.

Kettleborough, R.N., Busch-Nentwich, E.M., Harvey, S.A., Dooley, C.M., de Bruijn, E., van Eeden, F., Sealy, I., White, R.J., Herd, C., Nijman, I.J., et al. (2013). A systematic genome-wide analysis of zebrafish protein-coding gene function. Nature *496*, 494–497.

Kikuta, H., Kanai, M., Ito, Y., and Yamasu, K. (2003). gbx2 Homeobox gene is required for the maintenance of the isthmic region in the zebrafish embryonic brain. Dev. Dyn. *228*, 433–450.

Kim, G.Y., Kim, H.Y., Kim, H.T., Moon, J.M., Kim, C.H., Kang, S., and Rhim, H. (2012a). HtrA1 is a novel antagonist controlling fibroblast growth factor (FGF) signaling via cleavage of FGF8. Mol. Cell. Biol. *32*, 4482–4492.

Kim, S.E., Coste, B., Chadha, A., Cook, B., and Patapoutian, A. (2012b). The role of Drosophila Piezo in mechanical nociception. Nature *483*, 209–212.

Kloosterman, W.P., Lagendijk, A.K., Ketting, R.F., Moulton, J.D., and Plasterk, R.H. (2007). Targeted inhibition of miRNA maturation with morpholinos reveals a role for miR-375 in pancreatic islet development. PLoS Biol. *5*, e203.

Kok, F.O., Gupta, A., Lawson, N.D., and Wolfe, S.A. (2014). Construction and application of site-specific artificial nucleases for targeted gene editing. Methods Mol. Biol. *1101*, 267–303.

Law, S.H., and Sargent, T.D. (2014). The serine-threonine protein kinase PAK4 is dispensable in zebrafish: identification of a morpholino-generated pseudophenotype. PLoS ONE *9*, e100268.

Lawson, N.D., and Weinstein, B.M. (2002). In vivo imaging of embryonic vascular development using transgenic zebrafish. Dev. Biol. *248*, 307–318.

Lawson, N.D., and Wolfe, S.A. (2011). Forward and reverse genetic approaches for the analysis of vertebrate development in the zebrafish. Dev. Cell *21*, 48–64.

Lee, P., Goishi, K., Davidson, A.J., Mannix, R., Zon, L., and Klagsbrun, M. (2002). Neuropilin-1 is required for vascular development and is a mediator of VEGF-dependent angiogenesis in zebrafish. Proc. Natl. Acad. Sci. USA *99*, 10470–10475.

Lele, Z., Bakkers, J., and Hammerschmidt, M. (2001). Morpholino phenocopies of the swirl, snailhouse, somitabun, minifin, silberblick, and pipetail mutations. Genesis *30*, 190–194.

Lin, N., Chang, K.Y., Li, Z., Gates, K., Rana, Z.A., Dang, J., Zhang, D., Han, T., Yang, C.S., Cunningham, T.J., et al. (2014). An evolutionarily conserved long noncoding RNA TUNA controls pluripotency and neural lineage commitment. Mol. Cell *53*, 1005–1019.

Majczenko, K., Davidson, A.E., Camelo-Piragua, S., Agrawal, P.B., Manfready, R.A., Li, X., Joshi, S., Xu, J., Peng, W., Beggs, A.H., et al. (2012). Dominant mutation of CCDC78 in a unique congenital myopathy with prominent internal nuclei and atypical cores. Am. J. Hum. Genet. *91*, 365–371.

Mangos, S., Lam, P.Y., Zhao, A., Liu, Y., Mudumana, S., Vasilyev, A., Liu, A., and Drummond, I.A. (2010). The ADPKD genes pkd1a/b and pkd2 regulate extracellular matrix formation. Dis. Model. Mech. *3*, 354–365.

Martyn, U., and Schulte-Merker, S. (2004). Zebrafish neuropilins are differentially expressed and interact with vascular endothelial growth factor during embryonic vascular development. Dev. Dyn. *231*, 33–42.

Meng, X., Noyes, M.B., Zhu, L.J., Lawson, N.D., and Wolfe, S.A. (2008). Targeted gene inactivation in zebrafish using engineered zinc-finger nucleases. Nat. Biotechnol. *26*, 695–701.

Moser, M., Yu, Q., Bode, C., Xiong, J.W., and Patterson, C. (2007). BMPER is a conserved regulator of hematopoietic and vascular development in zebrafish. J. Mol. Cell. Cardiol. *43*, 243–253.

Nasevicius, A., and Ekker, S.C. (2000). Effective targeted gene 'knockdown' in zebrafish. Nat. Genet. *26*, 216–220.

Nishibori, Y., Katayama, K., Parikka, M., Oddsson, A., Nukui, M., Hultenby, K., Wernerson, A., He, B., Ebarasi, L., Raschperger, E., et al. (2011). Glcci1 deficiency leads to proteinuria. J. Am. Soc. Nephrol. *22*, 2037–2046.

Nourizadeh-Lillabadi, R., Seilø Torgersen, J., Vestrheim, O., König, M., Aleström, P., and Syed, M. (2010). Early embryonic gene expression profiling of zebrafish prion protein (Prp2) morphants. PLoS ONE *5*, e13573.

Parsons, M.J., Campos, I., Hirst, E.M., and Stemple, D.L. (2002a). Removal of dystroglycan causes severe muscular dystrophy in zebrafish embryos. Development *129*, 3505–3512.

Parsons, M.J., Pollard, S.M., Saúde, L., Feldman, B., Coutinho, P., Hirst, E.M., and Stemple, D.L. (2002b). Zebrafish mutants identify an essential role for laminins in notochord formation. Development *129*, 3137–3146.

Pei, W., Williams, P.H., Clark, M.D., Stemple, D.L., and Feldman, B. (2007). Environmental and genetic modifiers of squint penetrance during zebrafish embryogenesis. Dev. Biol. *308*, 368–378.

Pham, V.N., Lawson, N.D., Mugford, J.W., Dye, L., Castranova, D., Lo, B., and Weinstein, B.M. (2007). Combinatorial function of ETS transcription factors in the developing vasculature. Dev. Biol. *303*, 772–783.

Pickart, M.A., Klee, E.W., Nielsen, A.L., Sivasubbu, S., Mendenhall, E.M., Bill, B.R., Chen, E., Eckfeldt, C.E., Knowlton, M., Robu, M.E., et al. (2006). Genome-wide reverse genetics framework to identify novel functions of the vertebrate secretome. PLoS ONE *1*, e104.

Quillien, A., Moore, J.C., Shin, M., Siekmann, A.F., Smith, T., Pan, L., Moens, C.B., Parsons, M.J., and Lawson, N.D. (2014). Distinct Notch signaling outputs pattern the developing arterial system. Development *141*, 1544–1552.

Ransom, D.G., Haffter, P., Odenthal, J., Brownlie, A., Vogelsang, E., Kelsh, R.N., Brand, M., van Eeden, F.J., Furutani-Seiki, M., Granato, M., et al. (1996). Characterization of zebrafish mutants with defects in embryonic hematopoiesis. Development *123*, 311–319.

Robu, M.E., Larson, J.D., Nasevicius, A., Beiraghi, S., Brenner, C., Farber, S.A., and Ekker, S.C. (2007). p53 activation by knockdown technologies. PLoS Genet. *3*, e78.

San Antonio, J.D., Zoeller, J.J., Habursky, K., Turner, K., Pimtong, W., Burrows, M., Choi, S., Basra, S., Bennett, J.S., DeGrado, W.F., and Iozzo, R.V. (2009). A key role for the integrin alpha2beta1 in experimental and developmental angiogenesis. Am. J. Pathol. *175*, 1338–1347.

Sander, J.D., Dahlborg, E.J., Goodwin, M.J., Cade, L., Zhang, F., Cifuentes, D., Curtin, S.J., Blackburn, J.S., Thibodeau-Beganny, S., Qi, Y., et al. (2011). Selection-free zinc-finger-nuclease engineering by context-dependent assembly (CoDA). Nat. Methods *8*, 67–69.

Sayer, J.A., Otto, E.A., O'Toole, J.F., Nurnberg, G., Kennedy, M.A., Becker, C., Hennies, H.C., Helou, J., Attanasio, M., Fausett, B.V., et al. (2006). The centrosomal protein nephrocystin-6 is mutated in Joubert syndrome and activates transcription factor ATF4. Nat. Genet. *38*, 674–681.

Schenck, A., Goto-Silva, L., Collinet, C., Rhinn, M., Giner, A., Habermann, B., Brand, M., and Zerial, M. (2008). The endosomal protein Appl1 mediates Akt substrate specificity and cell survival in vertebrate development. Cell *133*, 486–497.

Seeley, M., Huang, W., Chen, Z., Wolff, W.O., Lin, X., and Xu, X. (2007). Depletion of zebrafish titin reduces cardiac contractility by disrupting the assembly of Z-discs and A-bands. Circ. Res. *100*, 238–245.

Seidel, J.J., and Graves, B.J. (2002). An ERK2 docking site in the Pointed domain distinguishes a subset of ETS transcription factors. Genes Dev. *16*, 127–137.

Stainier, D.Y., Fouquet, B., Chen, J.N., Warren, K.S., Weinstein, B.M., Meiler, S.E., Mohideen, M.A., Neuhauss, S.C., Solnica-Krezel, L., Schier, A.F., et al. (1996). Mutations affecting the formation and function of the cardiovascular system in the zebrafish embryo. Development *123*, 285–292.

Stowe, T.R., Wilkinson, C.J., Iqbal, A., and Stearns, T. (2012). The centriolar satellite proteins Cep72 and Cep290 interact and are required for recruitment of BBS proteins to the cilium. Mol. Biol. Cell *23*, 3322–3335.

Su, C.Y., Kemp, H.A., and Moens, C.B. (2014). Cerebellar development in the absence of Gbx function in zebrafish. Dev. Biol. *386*, 181–190.

Summerton, J.E. (2007). Morpholino, siRNA, and S-DNA compared: impact of structure and mechanism of action on off-target effects and sequence specificity. Curr. Top. Med. Chem. *7*, 651–660.

Summerton, J., and Weller, D. (1997). Morpholino antisense oligomers: design, preparation, and properties. Antisense Nucleic Acid Drug Dev. *7*, 187–195.

Swift, M.R., Pham, V.N., Castranova, D., Bell, K., Poole, R.J., and Weinstein, B.M. (2014). SoxF factors and Notch regulate nr2f2 gene expression during venous differentiation in zebrafish. Dev. Biol. *390*, 116–125.

Tijssen, M.R., Cvejic, A., Joshi, A., Hannah, R.L., Ferreira, R., Forrai, A., Bellissimo, D.C., Oram, S.H., Smethurst, P.A., Wilson, N.K., et al. (2011). Genome-wide analysis of simultaneous GATA1/2, RUNX1, FLI1, and SCL binding in megakaryocytes identifies hematopoietic regulators. Dev. Cell *20*, 597–609.

Traver, D., Paw, B.H., Poss, K.D., Penberthy, W.T., Lin, S., and Zon, L.I. (2003). Transplantation and in vivo imaging of multilineage engraftment in zebrafish bloodless mutants. Nat. Immunol. *4*, 1238–1246.

Tse, W.K., Eisenhaber, B., Ho, S.H., Ng, Q., Eisenhaber, F., and Jiang, Y.J. (2009). Genome-wide loss-of-function analysis of deubiquitylating enzymes for zebrafish development. BMC Genomics *10*, 637.

Ulitsky, I., Shkumatava, A., Jan, C.H., Sive, H., and Bartel, D.P. (2011). Conserved function of lincRNAs in vertebrate embryonic development despite rapid sequence evolution. Cell *147*, 1537–1550.

van Impel, A., Zhao, Z., Hermkens, D.M., Roukens, M.G., Fischer, J.C., Peterson-Maduro, J., Duckers, H., Ober, E.A., Ingham, P.W., and Schulte-Merker, S. (2014). Divergence of zebrafish and mouse lymphatic cell fate specification pathways. Development *141*, 1228–1238.

Vettori, A., Bergamin, G., Moro, E., Vazza, G., Polo, G., Tiso, N., Argenton, F., and Mostacciuolo, M.L. (2011). Developmental defects and neuromuscular alterations due to mitofusin 2 gene (MFN2) silencing in zebrafish: a new model for Charcot-Marie-Tooth type 2A neuropathy. Neuromuscul. Disord. *21*, 58–67.

Wiens, K.M., Lee, H.L., Shimada, H., Metcalf, A.E., Chao, M.Y., and Lien, C.L. (2010). Platelet-derived growth factor receptor beta is critical for zebrafish intersegmental vessel formation. PLoS ONE *5*, e11324.

Yao, S., Qian, M., Deng, S., Xie, L., Yang, H., Xiao, C., Zhang, T., Xu, H., Zhao, X., Wei, Y.Q., and Mo, X. (2010). Kzp controls canonical Wnt8 signaling to modulate dorsoventral patterning during zebrafish gastrulation. J. Biol. Chem. *285*, 42086–42096.

Yoo, S.K., Deng, Q., Cavnar, P.J., Wu, Y.I., Hahn, K.M., and Huttenlocher, A. (2010). Differential regulation of protrusion and polarity by PI3K during neutrophil motility in live zebrafish. Dev. Cell *18*, 226–236.

Yue, R., Kang, J., Zhao, C., Hu, W., Tang, Y., Liu, X., and Pei, G. (2009). Beta-arrestin1 regulates zebrafish hematopoiesis through binding to YY1 and relieving polycomb group repression. Cell *139*, 535–546.

Zhu, C., Smith, T., McNulty, J., Rayla, A.L., Lakshmanan, A., Siekmann, A.F., Buffardi, M., Meng, X., Shin, J., Padmanabhan, A., et al. (2011). Evaluation and application of modularly assembled zinc-finger nucleases in zebrafish. Development *138*, 4555–4564.

Zoeller, J.J., McQuillan, A., Whitelock, J., Ho, S.Y., and Iozzo, R.V. (2008). A central function for perlecan in skeletal muscle and cardiovascular development. J. Cell Biol. *181*, 381–394.